BIOCHEMISTRY
including biophysical chemistry & molecular biology

ARTICLE

pubs.acs.org/biochemistry

Modulation of Heme Orientation and Binding by a Single Residue in Catalase HPII of *Escherichia coli*

Vikash Jha,[†] Sherif Louis,[†] Prashen Chelikani,[†] Xavi Carpena,[‡] Lynda J. Donald,[†] Ignacio Fita,[‡] and Peter C. Loewen*[,†]

[†]Department of Microbiology, University of Manitoba, Winnipeg, MB R3T 2N2, Canada

[‡]Institute of Research in Biomedicine (IRB-Barcelona) and Institut de Biología Molecular (IBMB-CSIC), Parc Científic, Baldiri Reixac 10, 08028 Barcelona, Spain

Supporting Information

ABSTRACT: Heme-containing catalases have been extensively studied, revealing the roles of many residues, the existence of two heme orientations, flipped 180° relative to one another along the propionate−vinyl axis, and the presence of both heme *b* and heme *d*. The focus of this report is a residue, situated adjacent to the vinyl groups of the heme at the entrance of the lateral channel, with an unusual main chain geometry that is conserved in all catalase structures so far determined. In *Escherichia coli* catalase HPII, the residue is Ile274, and replacing it with Gly, Ala, and Val, found at the same location in other catalases, results in a reduction in catalytic efficiency, a reduced intensity of the Soret absorbance band, and a mixture of heme orientations and species. The reduced turnover rates and higher H_2O_2 concentrations required to attain equivalent reaction velocities are explained in terms of less efficient containment of substrate H_2O_2 in the heme cavity arising from easier escape through the more open entrance to the lateral channel created by the smaller side chains of Gly and Ala. Inserting a Cys at position 274 resulted in the heme being covalently linked to the protein through a Cys−vinyl bond that is hypersensitive to X-ray irradiation being largely degraded within seconds of exposure to the X-ray beam. Two heme orientations, flipped along the propionate−vinyl axis, are found in the Ala, Val, and Cys variants.

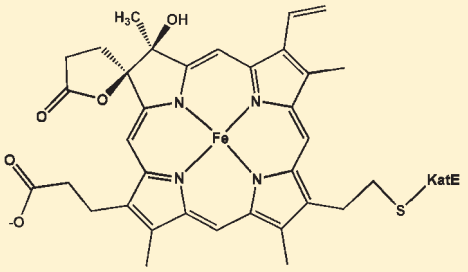

Heme-containing monofunctional catalases catalyze the degradation of H_2O_2 utilizing the hydroperoxide as both an oxidant of the heme (reaction 1) and a reductant of the intermediate oxoferryl heme species (reaction 2), both reactions being energetically favorable.

$$H_2O_2 + Por - Fe^{III} \rightarrow Por^{+\bullet}Fe^{IV}{=}O + H_2O \quad (1)$$

$$H_2O_2 + Por^{+\bullet}{-}Fe^{IV}{=}O \rightarrow Por{-}Fe^{III} + H_2O + O_2 \quad (2)$$

Several features of catalases have been identified as being important for catalysis, including specific residues and topographical features such as access channels. For example, a His and an Asn[1−3] in the distal side heme pocket and an Asp 12 Å[4] from the heme in the main channel are essential for or greatly enhance the catalytic process. The dimensions of the access channels, as determined by the residues lining them, are similarly important.[5] For example, removal of an Arg-Glu pair in the lateral channel enhanced activity almost 3-fold,[6] presumably because the enlarged channel allowed easier movement of substrate H_2O_2 and products O_2 and H_2O.

Modifications of amino acids and the heme, usually arising from oxidations, are common in catalases. In addition to there being two different heme orientations among the catalases, some large subunit or clade 2 catalases contain heme *d*, in which one propionate is converted to a hydroxylated spirolactone.[2,7] In *Escherichia coli* catalase HPII (also KatE), the proximal ligand Tyr415 is covalently linked to the nearby His392,[8] while in *Neurospora crassa* Cat1, the Tyr-His linkage is replaced by a Tyr-Cys link.[9] Catalases generally have a small number of cysteines, and their modification in KatE has been reported.[10] Surprisingly, none of these modifications are required for or significantly affect activity, but they may protect the enzyme against further oxidation and, by providing increased rigidity, may enhance the enzyme's heat and protease resistance.[11,12]

Among the 13 catalase structures so far determined, a small number of residues are found with unfavorable backbone geometry, but the location of one residue ($\psi \approx -60°$, and $\phi \approx 70°$) has been conserved across representatives from all three phylogenetic clades of the enzyme. The location of this residue is near the heme edge at the opening to the lateral channel (Figure 1), an access route to the heme cavity that also parallels an electron transfer route between NADPH and the heme in some small subunit clade 3 enzymes.[13,14] Only five different amino acids are found at the location among all catalases, including Val (62%), Ser (32%), Gly (3%), Ile (2%), and Ala (1%), with Ile being found only in large subunit clade 2 catalases, including Ile274

Received: September 29, 2010
Revised: February 18, 2011
Published: February 18, 2011

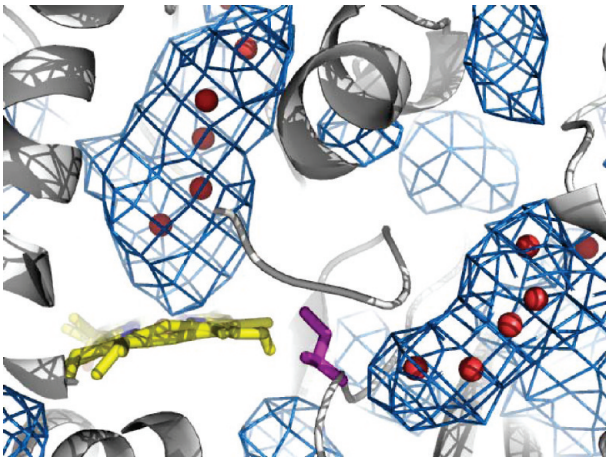

Figure 1. View of the heme cavity in HPII in relation to the main and lateral access channels based on the coordinates in PDB entry 1GGE.[3] The heme is colored yellow and the side chain of I274 magenta. The periphery or surface of the channels is indicated by the blue mesh, and the red spheres within the mesh mark the locations of waters in the channels. The main channel is perpendicular to the plane of the heme, and the lateral channel extends to the right with the I274 side chain situated at its end.

in *E. coli* catalase HPII. Serine at the location has been assigned a role in the transfer of an electron from NADPH to heme,[14] and the slow turnover rates of large subunit catalases have been correlated, in part, with the presence of isoleucine blocking the entrance to the lateral channel.[6,15]

To define more clearly the role of this location, whether catalytic, structural, or both, we constructed and characterized a series of variants of *E. coli* catalase HPII mutated at position 274. Changes in catalytic efficiency attributable, in part, to less effective containment of the substrate H_2O_2 and changes in the heme orientation revealed the importance of the residue in maintaining the catalytic and structural integrity of the enzyme. In addition, a covalent cross-link between the heme and protein was found in the I274C variant.

METHODS

Construction, Purification, and Characterization of Variant Proteins. Standard chemicals and biochemicals were obtained from Sigma. Oligonucleotides GGCTTCGGTGCTCACACCTTC (I274A), GGCTTCGGTGGTCACACCTTC (I274G), GGCTTCGGTGTTCACACCTTC (I274V), GGCTTCGGTTTTCACACCTTC (I274F), and GGCTTCGGTAGTCACACCTTC (I274S) were purchased from Invitrogen and used to mutate the *Hin*dIII−*Eco*RI fragment (base pairs 1246−1856) of pAMkatE72[16] following the Kunkel procedure[17] as previously described.[4] Oligonucleotide GGCTTCGGTTGCCACACCTTC (I274C) was used to mutate the same fragment from a previously constructed variant, pC438A/C669A, in which both cysteines had been mutated to alanine.[10] The mutated sequences were confirmed[18] and used to generate plasmids pI274A, pI274G, pI274V, pI274C, pI274S, and pI274F via reincorporation of the fragment into the full-length *katE* gene. The native and variant proteins were expressed and purified as described previously.[4] Catalase activity was determined by the method of Rørth and Jensen[19] in a Gilson oxygraph equipped with a Clark electrode. One unit of catalase is defined as the amount that decomposes 1 μmol of H_2O_2 in 1 min in a 60 mM H_2O_2 solution at pH 7.0 and 37 °C. The initial rates of oxygen evolution were used to determine the turnover rates to minimize inactivation caused by high H_2O_2 concentrations. Protein was estimated according to the methods outlined by Layne.[20] All spectra were recorded using a Milton Roy MR3000 spectrophotometer.

Table 1. Kinetic Constants for the I274 Variants of *E. coli* Catalase HPII

	specific activity[a]	k_{cat} (s^{-1})	K_M (app)[b] (mM)	R_Z[c]	heme *d*[d]	heme *b*[d]
native	19000 ± 900	100800	220	0.98	+	−
I274G	4300 ± 710	13700	1000	0.52	+	+
I274A	7700 ± 490	20900	500	0.74	+	+
I274V	18000 ± 1400	53000	500	0.97	+	+
I274C	4560 ± 600	19300	80	0.52	+	+

[a] Specific activity, in units per milligram of protein. [b] K_M(app) is the H_2O_2 concentration at $V_{max}/2$. [c] $R_Z = A_{407}/A_{280}$. [d] The presence (+) or absence (−) of heme *d* and heme *b* was determined by absorbance bands at 590 nm (heme *d*) or 630 nm (heme *b*) and by HPLC after acetone-HCL extraction (except for I274C).

Crystallization and Structure Determination. Crystals of the I274 variants were obtained at 22 °C using the hanging drop vapor diffusion method over a reservoir solution containing 15−17% PEG 3350 (Carbowax), 1.6−1.7 M LiCl, and 0.1 M Tris (pH 9.0).[21,22] The crystals were monoclinic in space group $P2_1$ with one tetrameric molecule in the crystal asymmetric unit. Data sets were collected using synchrotron beamline CMCF 08ID-1 at the Canadian Light Source in Saskatoon, SK, from crystals flash-cooled in reservoir buffer. Diffraction data were processed and scaled using MOSFLM and SCALA,[23] respectively (Table 2). To obtain a picture of changes occurring as a result of X-ray irradiation, blocks of six images (1−6, 7−12, 13−18, etc.) from 33 different crystals were merged into single data sets using SCALA. Structure refinement starting with the native KatE structure (PDB entry 1GGE) was completed using REFMAC[24] and manual modeling with the molecular graphics program COOT.[25] The Ramachandran distribution of residues for all structures was ~96, 3.5, and 0.5% in the favored, allowed, and outlier regions, respectively. Figures were generated using PYMOL (The PYMOL Molecular Graphics System, Schrödinger, LLC).

RESULTS

Construction and Characterization of I274 Variants. Residue Ile274 in *E. coli* catalase HPII is situated adjacent to the heme edge at the entrance to the lateral channel and, like residues at the same position in other catalases, possesses an unfavorable main chain geometry. To investigate the integrity of this residue in the catalytic function of the enzyme, it was mutated to residues found at the same location in other catalases. Specifically, plasmids harboring mutated *katE* genes encoding I274V, I274S, I274A, and I274G were constructed, along with genes encoding I274C, to provide a sulfhydryl group for the introduction of nonstandard amino acid side chains, and I274F, to insert a large aromatic group.

Despite repeated attempts, no protein was ever obtained from the I274S or I274F construct. This was most likely the result of aberrant folding that allowed proteolysis to occur before a protease resistant structure was formed.[26] While not a big

Table 2. Data Collection and Refinement Statistics

		Data Collection		
variant	I274G	I274A	I274V	I274C
PDB entry	3P9R	3P9S	3P9P	3P9Q
unit cell parameters				
a (Å)	93.41	93.56	93.50	93.66
b (Å)	133.18	133.17	132.82	133.02
c (Å)	122.74	122.81	122.59	122.59
α, *γ* (deg)	90.0	90.0	90.0	90.0
β (deg)	109.21	109.24	109.47	109.60
resolution[a]	35.2−1.90 (2.00−1.90)	31.3−1.90 (2.00−1.90)	29.4−1.50 (1.58−1.50)	35.2−1.48 (1.52−1.48)
no. of unique reflections	221203 (31939)	197718 (23877)	426044 (58221)	429958 (54412)
completeness (%)	99.4 (98.7)	88.9 (74.0)	95.0 (89.1)	91.8 (79.7)
R_{merge}	0.139 (0.533)	0.097 (0.284)	0.119 (0.590)	0.081 (0.483)
$\langle I/\sigma I \rangle$	8.7 (2.9)	7.5 (3.1)	7.0 (1.9)	8.4 (2.0)
multiplicity	3.8 (3.7)	2.8 (2.2)	3.7 (3.1)	3.1 (2.7)
		Model Refinement		
no. of reflections	210008	187606	404546	408282
R_{cryst} (%)	13.3	13.7	14.9	14.3
R_{free} (%)	18.4	19.1	18.5	17.8
no. of non-H atoms	26363	26530	26643	26893
no. of water molecules	3196	3183	3269	3496
average *B* factor (Å^2)				
protein	14.2	13.9	12.8	13.2
heme	11.4	6.3	3.8	8.5
waters	24.0	21.5	23.9	23.0
other				
coordinate error (Å)[b]	0.082	0.085	0.046	0.042
rmsd for bonds (Å)	0.024	0.024	0.027	0.029
rmsd for angles (deg)	1.90	2.00	2.34	2.36

[a] Values in parentheses correspond to the highest-resolution shell. [b] Based on maximum likelihood.

surprise in the case of I274F, where the large phenyl ring would have occluded heme packing and interfered with protein folding, the outcome with I274S was puzzling because Ser is common at this location among catalases, is similar in size to the Cys in I274C, and is smaller than the *β*-branched I274V and native I274, all of which accumulated normal amounts of protein along with I274G and I274A.

The kinetic parameters of the Gly, Ala, and Val variants reveal reduced turnover rates and decreased affinities for H_2O_2 (higher apparent K_M values) (Table 1), leading to a correlation of lower activity with smaller residues at position 274, just the opposite of what was expected for a less obstructed entrance to the lateral channel. The Cys variant also exhibits a slower turnover rate and differed only in presenting a reduced apparent K_M, which may be related to cysteine-specific reactions described below. The term "apparent K_M" [K_M(app)] in the context of catalases is the H_2O_2 concentration at $V_{max}/2$ and is used because the catalatic reaction does not saturate with substrate and therefore does not precisely follow Michaelis−Menten kinetics.[15]

Extraction of heme from the variants by acetone-HCl followed by HPLC analysis revealed predominantly heme *d*, the heme normally found in HPII, but with amounts of heme *b* that varied from batch to batch with even the native enzyme containing some heme *b*. The presence of heme *b* was also confirmed by its characteristic 630 nm band in the absorbance spectra (Table 1). I274C was unique in yielding no extractable heme either by acetone-HCl extraction or during mass spectrometry analysis (Figures S1 and S2 of the Supporting Information), suggesting that its heme was covalently linked to the protein.

The A_{407}/A_{280} ratio or R_Z is commonly used as a measure of protein purity and heme content. For native HPII, the pure enzyme exhibits an R_Z of ∼1.0, consistent with its aromatic amino acid content, but the R_Z values exhibited by I274A, I274G, and I274C are much lower, in the range of 0.5−0.6, similar to what has previously been reported for the Cpd I/II derivative of native HPII.[27] Two explanations for such low values, impure protein or low heme content, are inconsistent with the >95% purity as judged by sodium dodecyl sulfate−polyacrylamide gel electrophoresis and the integrity of the heme in the core of the enzyme that precludes protein folding in its absence. In the case of I274C, an additional charge transfer band at 670 nm is evident, suggesting a change in heme chemistry.

Crystal Structure Analysis of the I274 Variants. To determine what changes in structure might be responsible for the catalytic and spectral differences observed among the I274 variants, we determined their structures by X-ray crystallography. Crystals of I274G, I274A, I274V, and I274C were prepared and used to collect X-ray diffraction data sets that refined between 1.9 and 1.5 Å (Table 2). The electron density maps clearly defined the main chain and side chain atoms of 2904 amino acids, four heme groups, and 3200−3500 waters in four subunits. As in the native structure, the 28 N-terminal residues are not visible, but

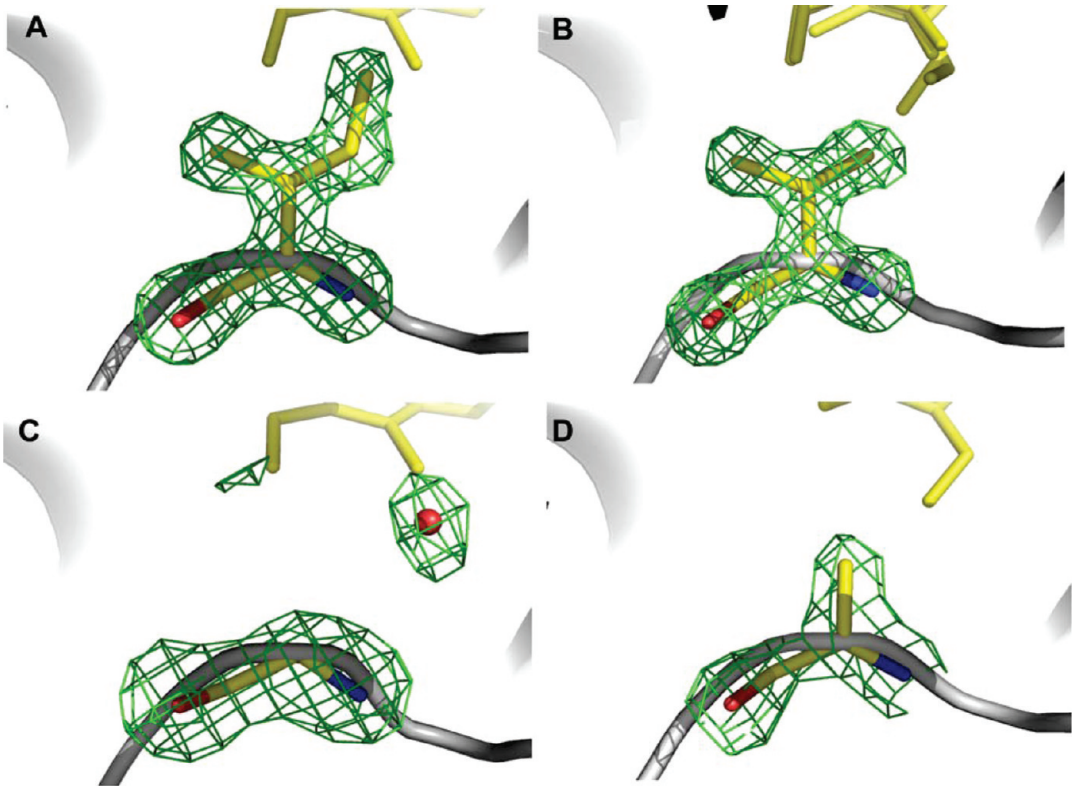

Figure 2. Electron density maps corresponding to the side chains of Ile274 (A), Val274 (B), Gly274 (C), and Ala274 (D). The $F_o - F_c$ electron density maps, colored green at 3.0σ, were calculated without the side chain in the model, and the appropriate models are superimposed.

the maps show complete continuity from Ser28 to Ala753 in all four subunits. The expected side chains at position 274 were evident for I274A, I274G, and I274V (Figure 2), and the unfavorable geometry of the residue was retained in each. A new water in the cavity created by the missing side chain was evident in I274G, coordinated between the main chain carbonyl oxygens of Thr203 (2.9 Å) and Phe272 (3.5 Å) (Figure 2C). In all three cases, the covalent linkage between the side chains of Tyr415 and His392 was fully formed, confirming that the variants had gone through several rounds of catalysis prior to purification.[2] In addition, the crystal structures of the variants reveal distal side waters coordinated with the heme iron at higher occupancies in I274A, I274C, and I274G than in I274V or the native enzyme (Figure 3).

Heme Heterogeneity. The heme of catalases is either heme *b* or heme *d* and is found in one of two orientations that are "flipped" along the vinyl−propionate axis relative to one another. In native HPII, a mixture of heme *b* and heme *d* is always found with heme *d* or heme *b* predominating (>80%) in cells grown aerobically[28] or anaerobically,[2] respectively. In native HPII and catalase CatF from *Pseudomonas syringae*,[29] the heme is oriented with ring IV overlapping or stacked (3.4 Å) with the imidazole ring of the essential histidine (His128 in HPII), the His-IV orientation. The opposite or flipped orientation with ring III stacked with the essential histidine (His-III) is found in clade 3 enzymes.[1,5,30,31] It was therefore surprising to find a mixture of approximately equal proportions of both orientations in I274V and a greater proportion of the flipped, His-III, orientation in I274A (Figure 4). The orientation and relative amounts were estimated on the basis of satisfactory refinements with partial occupancies of the two orientations and the *B* factors for the vinyl C_β atoms being similar to those of the nearby heme atoms. The presence of predominantly His-IV orientation in I274G breaks the apparent correlation of more His-III orientation with smaller side chains, but this discrepancy might be explained by the water apparently replacing the side chain (Figure 2C). In this location, it is 3.6 Å from the ring I methyl in the His-IV orientation and would make contact with a vinyl at that location in the His-III orientation. Thus, while the identity of residue 274 in the proximity of the heme vinyl groups does influence heme orientation, chain size is not the only determinant. I274A also presents an unusual modification on the vinyl, possibly a result of hydroxylation (Figure 4D). A water refines nicely at this location ~1.7 Å from the vinyl carbon, but confirmatory data are needed.

The heme complement in I274V includes both orientations of both heme *d* and heme *b*, estimated to be in equal proportions on the basis of a comparison of *B* factors of the spirolactone and unmodified propionate atoms. This would have arisen from heme *b* initially binding in both orientations, each of which would have been oxidized stereospecifically to generate the two different isomers of heme *d*. In the native His-IV orientation, carbons 12 and 13 of ring III are modified to the 12(*S*)-hydroxy-13(*R*)-*cis*-spirolactone porphyrin, whereas in the flipped His-III orientation, carbons 17 and 18 of ring IV are modified to an 18(*S*)-hydroxy-17(*R*)-*cis*-spirolactone porphyrin (Figure 4E,F). The subtlety of these stereochemical differences is illustrated by the fact that the initial structural assignment of heme *d* from HPII based on NMR was as 12(*R*)-hydroxy-13(*S*)-*cis*-spirolactone,[32] and this was later revised by the X-ray structure to the 12(*S*),13-(*R*) isomer in both HPII and *Penicillium vitale* catalase.[7] The native crystal (Figure 4A) also shows evidence of a small amount of heme *b*, confirming that the extent of heme *b* to heme *d*

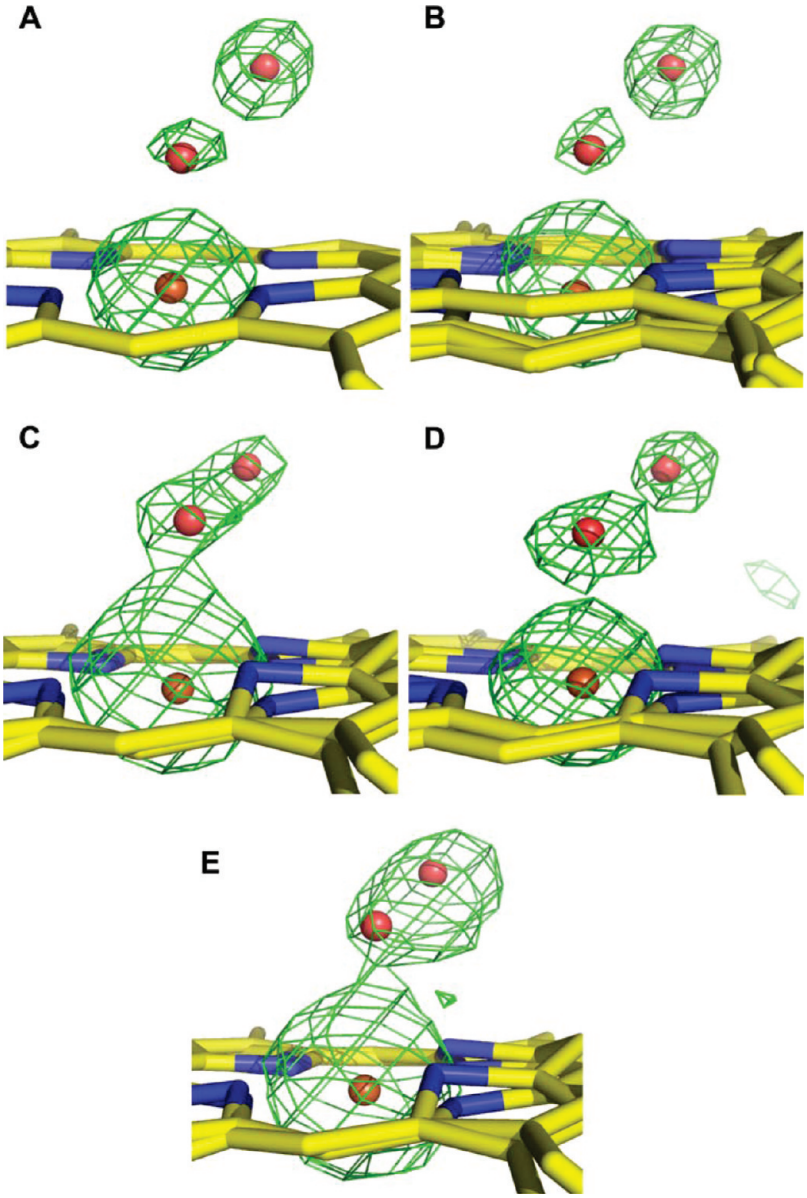

Figure 3. Electron density maps showing the heme iron and distal side waters in the native enzyme (A), I274V (B), I274A (C), I274C (D), and I274G (E). The $F_o - F_c$ electron density maps, colored green at 3.0σ, were calculated without iron or oxygen in the model, and the orange sphere for iron and the red sphere for oxygen are superimposed for the sake of illustration. The multiplicity of different heme orientations is also included.

conversion is batch-specific and must be determined by subtle differences in growth conditions.

X-ray Irradiation Causes Changes in the Structure of I274C. Analysis of the I274C diffraction data was presumably complicated by chemical changes associated with a striking color change in the crystal from the normal dark brown-green to bright green that occurred rapidly upon exposure to an X-ray beam (Figure 5). Fortunately, the chemical changes causing the color change did not affect the diffraction quality of the crystals, which routinely diffracted to >1.6 Å (Table 2).

The electron density maps reveal only heme *d*, but with approximately equal proportions of the two orientations. Unlike the I274G, I274A, and I274V variants, which produced electron density maps that were readily satisfied by the expected side chains in the model, a cysteine side chain presents only a partial solution for residue 274 in I274C. The $2F_o - F_c$ omit maps present four unusual features, including (i) the presence of weak density corresponding to C_β, (ii) a sphere of density close to but only weakly linked to either the heme vinyl or the C_β atom of residue 274, (iii) a nearby isolated sphere of density, and (iv) density between the heme vinyl and the side chain of Asn201 (Figure 6A). Whereas Figure 6A shows no obvious electron density linking the vinyl group (in the His-III orientation) and Cys274, the maps in Figure 6B (the orientation is rotated to that in Figure 4) calculated from a data set of early images (see below and Table 3) reveal density linking the protein with the vinyl of the heme, although both bonds are somewhat stretched, 1.9 Å for the C_β−S bond and 1.7 Å for the heme−S bond. The unlinked sulfur is situated approximately 2.5 Å from the heme vinyl (in the His-IV orientation) and 2.2 Å from the C_β methylene group, too far in both cases for the formation of a covalent bond. Given that the heme is 100% covalently attached to the protein before X-ray

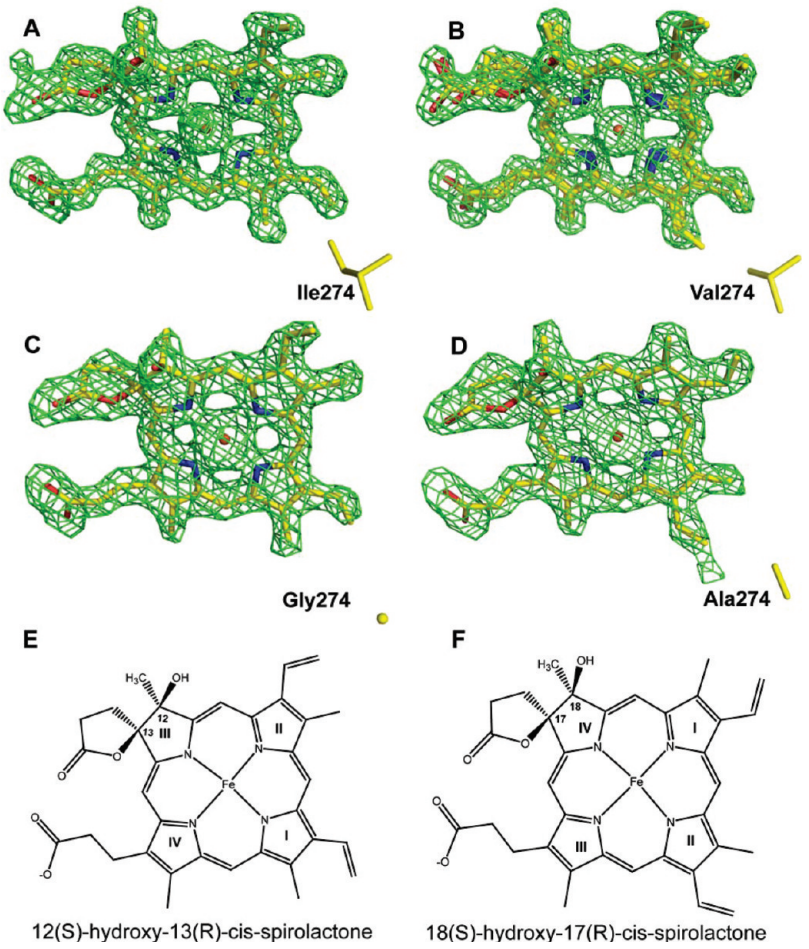

Figure 4. Heme composition in the native HPII (A), I274V (B), I274G (C), and I274A (D). The side chains of the different residues are shown at the bottom right of each panel for orientation. The $F_o - F_c$ electron density maps, colored green at 3.0σ, were calculated without heme in the model, and the appropriate models are superimposed for the sake of illustration. The native enzyme (A) and I274G variant (C) contain predominantly the His-IV orientation. The I274V variant (B) contains a mixture of heme *b* and heme *d* in both the native His-IV and flipped His-III orientations, while the I274A variant contains predominantly (~70%) heme *d* in the flipped His-III orientation. The stereochemistry of the heme D isomers is shown for the native His-IV orientation in panel E and the flipped His-III orientation in panel F.

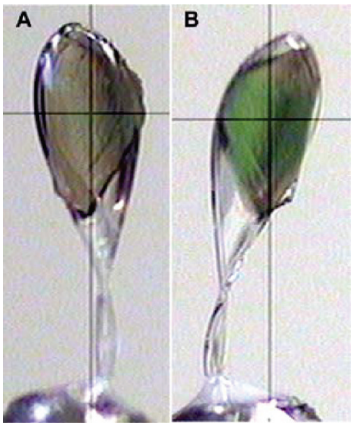

Figure 5. Color change in a crystal of I274C before (A) and after (B) X-ray irradiation.

exposure, these maps suggest that the covalent bonds between the Cys S and the nearby vinyl groups, 50% in each orientation, are very sensitive to X-ray irradiation. The covalent bond that would have existed between what has become the unlinked sulfur and the heme is more sensitive than that between the residual Cys and the heme, for which there is stronger density. Another unusual and unexpected feature evident in the electron density maps is the presence of weak density linking the heme and the distal side asparagine (N201) (Figure 6A).

The rapid color change caused by X-ray irradiation suggested that changes in heme chemistry were occurring within the first one or two exposures to the X-ray beam, whereas the fragmented model evident in the refined structure (Figure 6A) was initially based on a data set of 180 sequential images. In an attempt to gain a better picture of the molecule before X-ray damage had occurred, images from 33 different crystals were merged in blocks of six (images 1−6, 7−12, 13−18, etc.) (Table 3). There was more evidence of the Cys−heme cross-link in the electron density maps calculated from the first six images (Figure 6B), but there is still considerable breakage evident, particularly around the unlinked sulfur atom. Further degradation of the Cys−heme bond is evident as exposure times increase until there is no further bond evident after 30 exposures (Figure S3 of the Supporting Information). In addition, the density between the heme and Asn201 is not

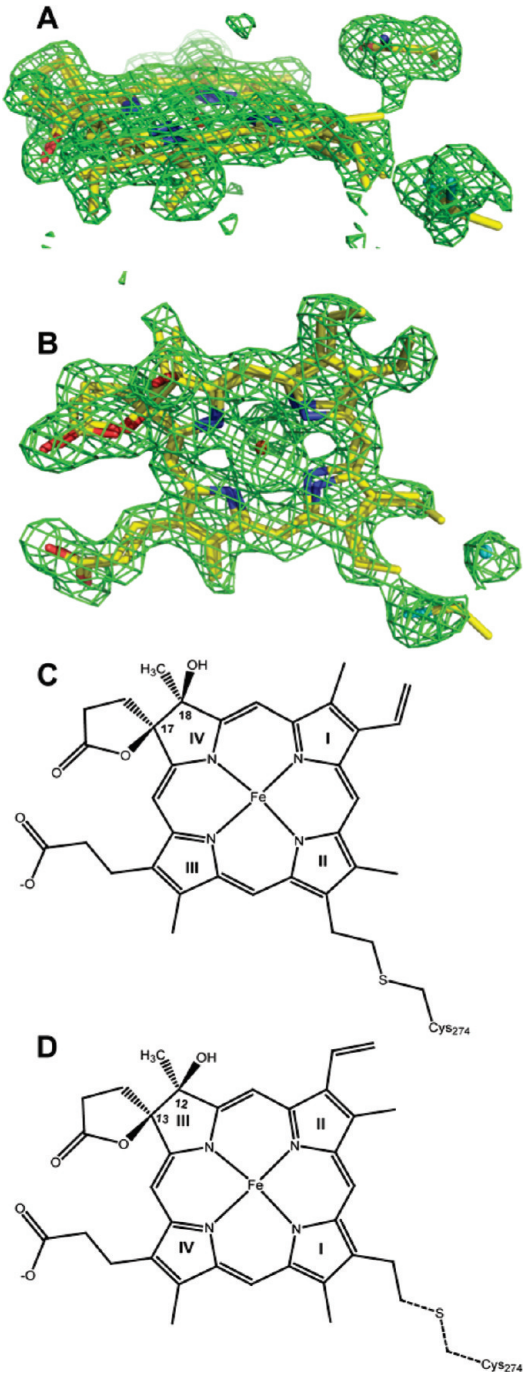

Figure 6. Electron density maps illustrating the residual heme−protein cross-link in I274C. The $F_o - F_c$ electron density maps, colored green at 3.0σ, were calculated without heme in the model, and the appropriate models are superimposed for the sake of illustration. Two different views are shown in panels A and B. The electron density maps in panel A were calculated from a complete data set and reveal the absence of density between the heme and Cys side chains. In addition, the weak density approaching the distal side Asn201 is evident. The maps in panel B were calculated from a merged data set of the first six images (1−6) from 33 crystals and are shown in the same orientation as in Figure 3 for comparison with the other variants. Panels C and D show the structures of the two different heme−Cys cross-links arising from the presence of two heme D isomers. The structure in panel D is shown with dashed bonds because the linkage has been completely destroyed by irradiation, whereas there is weak electron density evidence for the structure in panel C.

evident at short exposure times, indicating that it is a result of longer X-ray exposure

DISCUSSION

Changing the side chain of Ile274 in HPII, a residue with unusual main chain geometry located in the heme cavity at the entrance to the lateral channel, elicits a number of changes in the activity and structure of the enzyme, including reduced turnover rates, a mixture of heme orientations, and heme cross-linking to the protein in the Cys variant. Previous work had demonstrated that enlarging the middle section of the lateral channel led to an increase in activity,[6] leading to the hypothesis that opening the entrance to the lateral channel would also enhance activity. In fact, just the opposite is observed, with catalytic efficiency decreasing as the channel is opened, and an explanation may lie in the recent prediction arising from a computational study that the heme cavity has evolved to restrict efflux of H_2O_2, thereby extending its residency time in the cavity.[33] Thus, the bulky isoleucine in the native enzyme restricts movement of H_2O_2 out of the cavity via the lateral channel, and the longer occupancy in the cavity increases its chances of participating in the reaction. Conversely, opening the lateral channel (with smaller side chains at residue 274) facilitates diffusion of H_2O_2 out of the cavity, leading to a shorter residency time, poorer substrate binding, and a slower reaction. The elevated apparent K_M values for H_2O_2 exhibited by the I274G, I274A, and I274V variants suggest that higher substrate concentrations are required for equivalent turnover rates and are consistent with this explanation. The slower turnover rate of I274C may also be influenced by heme oxidation inherent in the Cys−heme cross-link, which may affect the reduction potentials of the heme and its Cpd I intermediate.

The increased heme heterogeneity cannot be so easily rationalized. Reducing the size of the side chain from isobutyl (I274) to isopropyl (I274V) or methyl (I274A) seems to remove a determinant that restricts heme binding to the orientation with the essential histidine stacked above ring IV of the heme found in native KatE. Approximately equal proportions of the native His-IV and flipped His-III orientations of heme are found in I274V, and a predominance of the flipped orientation is evident in I274A. I274G breaks the apparent correlation of a smaller subunit with the flipped His-III orientation, possibly a result of a water occupying the enlarged cavity. Partial conversion of heme *b* to heme *d*, a result of small changes in growth conditions, and not the type of mutation, results in an even more complex heme composition with the different heme types in two different orientations. Furthermore, whereas heme *b* is identical in both orientations, the flipped orientations of heme *d* are actually stereochemically distinct isomers, 12(*S*)-hydroxy-13(*R*)-*cis*-spirolactone in the native His-IV orientation and 18(*S*)-hydroxy-17(*R*)-*cis*-spirolactone in the flipped His-III orientation.

The covalent cross-link between the cysteine and heme in I274C is reminiscent of the outcome from the mutation of Val169 to Cys at the entrance of the main channel into the heme cavity which resulted in a Cys169−His128 cross-linked structure.[28] In both cases, the strategy of chemically introducing groups by sulfhydryl modification had to be abandoned because of the highly oxidative environment of the heme active site. The color change in the crystal after just seconds of exposure and the fact that images after six exposures show only limited evidence of

Table 3. Data Collection and Refinement Statistics

Data Collection							
image range	1−6	7−12	13−18	19−24	25−30	31−36	37−42
PDB entry	3PQ2	3PQ3	3PQ4	3PQ5	3PQ6	3PQ7	3PQ8
unit cell parameters							
a (Å)	93.51	93.51	93.51	93.50	93.50	93.50	93.50
b (Å)	133.03	133.03	133.03	133.02	133.02	133.02	133.02
c (Å)	122.65	122.65	122.65	122.68	122.67	122.67	122.67
α, *γ* (deg)	90.0	90.0	90.0	90.0	90.0	90.0	90.0
β (deg)	109.39	109.39	109.39	109.40	109.40	109.40	109.40
resolution[a]	35.3−1.8 (1.9−1.8)	35.3−1.8 (1.9−1.8)	35.3−1.8 (1.9−1.8)	35.2−1.8 (1.9−1.8)	35.2−1.8 (1.9−1.8)	35.2−1.8 (1.9−1.8)	35.2−1.8 (1.9−1.8)
no. of unique reflections	243208 (34037)	243581 (34062)	242816 (33840)	244091 (33699)	243484 (33500)	243516 (33926)	247243 (34670)
completeness (%)	93.0 (89.4)	93.1 (89.4)	92.8 (88.8)	93.4 (98.5)	93.1 (87.9)	93.1 (89.1)	94.5 (91.0)
R_{merge}	0.161 (0.428)	0.159 (0.419)	0.157 (0.430)	0.148 (0.370)	0.146 (0.367)	0.147 (0.379)	0.155 (0.412)
$\langle I/\sigma I \rangle$	7.9 (3.3)	7.9 (3.2)	7.9 (3.2)	7.8 (3.2)	6.4 (2.7)	7.4 (3.2)	7.5 (3.3)
multiplicity	3.5 (3.1)	3.5 (3.2)	3.5 (3.2)	3.2 (2.8)	3.1 (2.7)	3.1 (2.8)	3.1 (2.9)
Model Refinement							
no. of reflections	230767	231142	230481	231647	231011	231079	234622
R_{cryst} (%)	14.2	14.2	14.1	14.3	14.3	14.2	14.3
R_{free} (%)	18.9	18.9	18.9	19.0	19.1	19.0	19.0
no. of non-H atoms	26834	26828	26821	26829	26815	26809	26810
no. of water molecules	3445	3442	3435	3443	3429	3423	3424
average *B* factor (Å^2)							
protein	12.4	12.6	12.4	12.8	12.8	12.9	13.2
heme	6.7	7.1	7.2	7.0	7.3	7.6	7.4
waters	22.7	23.1	23.5	23.4	23.5	23.5	23.8
other							
coordinate error (Å)[b]	0.070	0.075	0.071	0.071	0.071	0.071	0.071
rmsd for bonds (Å)	0.024	0.024	0.025	0.025	0.025	0.024	0.025
rmsd for angles (deg)	1.96	2.00	2.02	2.03	2.02	2.02	2.03

[a] Values in parentheses correspond to the highest-resolution shell. [b] Based on maximum likelihood.

dx.doi.org/10.1021/bi200027v |*Biochemistry* 2011, 50, 2101–2110

the cross-link speak to its hypersensitivity to X-ray irradiation. Such extreme sensitivity is surprising in light of the similar protein−heme cross-links found in myeloperoxidase,[34,35] cytochrome *c*,[36] and cytochrome P460[37] where they are stable to X-ray irradiation. Possible explanations for the sensitivity lie in the strained stereochemistry, evident in the slightly stretched nature of the bonds in the refined model, and in the involvement of heme *d* rather than heme *b*.

■ ASSOCIATED CONTENT

Supporting Information. Heme being released from HPII but not from the I274C variant (Figures S1 and S2) and the disappearance of electron density corresponding to the Cys−heme bond in the I274C variant as a function of an increasing level of X-ray irradiation (Figure S3). This material is available free of charge via the Internet at http://pubs.acs.org.

Accession Codes

The coordinates for the structures included here have been submitted as Protein Dara Bank entries 3P9P (I274V), 3P9Q (I274C), 3P9R (I274G), 3P9S (I274A), 3PQ2 (I274C images 1−6), 3PQ3 (I274C images 7−12), 3PQ4 (I274C images 13−18), 3PQ5 (I274C images 19−24), 3PQ6 (I274C images 25−30), 3PQ7 (I274C images 31−36), and 3PQ8 (I274C images 37−42).

■ AUTHOR INFORMATION

Corresponding Author

*Department of Microbiology, University of Manitoba, Winnipeg, MB R3T 2N2, Canada. Phone: (204) 797-2134. Fax: (204) 474-7603. E-mail: peter_loewen@umanitoba.ca.

Funding Sources

This work was supported by Discovery Grant 9600 from the Natural Sciences and Engineering Research Council of Canada (to P.C.L.), by the Canada Research Chair Program (to P.C.L.), and by Grant BFU2009-09268 from the Spanish Ministry of Science and Innovation (to I.F.). Research described in this paper was performed at the Canadian Light Source, which is supported by the Natural Sciences and Engineering Research Council of Canada, the National Research Council of Canada, the Canadian Institutes of Health Research, the Province of Saskatchewan, Western Economic Diversification Canada, and the University of Saskatchewan.

■ ABBREVIATIONS

HPII, hydroperoxidase II; R_Z, A_{407}/A_{280} ratio; PDB, Protein Data Bank; rmsd, root-mean-square deviation.

■ REFERENCES

(1) Fita, I., Silva, A. M., Murthy, M. R. N., and Rossmann, M. G. (1986) The refined structure of beef liver catalase at 2.5 Å resolution. *Acta Crystallogr. B42*, 497–515.

(2) Loewen, P. C., Switala, J., von Ossowski, I., Hillar, A., Christie, A., Tattrie, B., and Nicholls, P. (1993) Catalase HPII of *Escherichia coli* catalyzes the conversion of protoheme to cis-heme d. *Biochemistry 32*, 10159–10164.

(3) Melik-Adamyan, W., Bravo, J., Carpena, X., Switala, J., Maté, M. J., Fita, I., and Loewen, P. C. (2001) Substrate flow in catalases deduced from the crystal structures of active site variants of HPII from *Escherichia coli*. *Proteins 44*, 270–281.

(4) Chelikani, P., Carpena, X., Fita, I., and Loewen, P. C. (2003) An electrical potential in the access channel of catalases enhances catalysis. *J. Biol. Chem. 278*, 31290–31296.

(5) Putnam, C. D., Arvai, A. S., Bourne, Y., and Tainer, J. A. (2000) Active and inhibited human catalase structures: Ligand and NADPH binding and catalytic mechanism. *J. Mol. Biol. 296*, 295–309.

(6) Sevinc, M. S., Maté, M. J., Switala, J., Fita, I., and Loewen, P. C. (1999) Role of the lateral channel in catalase HPII of *Escherichia coli*. *Protein Sci. 8*, 490–498.

(7) Murshudov, G. N., Grebenko, A. I., Barynin, V., Dauter, Z., Wilson, K. S., Vainshtein, B. K., Melik-Adamyan, W., Bravo, J., Ferrán, J. M., Ferrer, J. C., Switala, J., Loewen, P. C., and Fita, I. (1996) Structure of the heme d of *Penicillium vitale* and *Escherichia coli* catalases. *J. Biol. Chem. 271*, 8863–8868.

(8) Bravo, J., Fita, I., Ferrer, J. C., Ens, W., Hillar, A., Switala, J., and Loewen, P. C. (1997) Identification of a novel bond between a histidine and the essential tyrosine in catalase HPII of *Escherichia coli*. *Protein Sci. 6*, 1016–1023.

(9) Díaz, A., Horjales, E., Rudiño-Piñera, E., Arreola, R., and Hansberg, W. (2004) Unusual Cys-Tyr covalent bond in a large catalase. *J. Mol. Biol. 342*, 971–985.

(10) Sevinc, M. S., Ens, W., and Loewen, P. C. (1995) The cysteines of catalase HPII of *Escherichia coli*, including Cys438 which is blocked, do not have a catalytic role. *Eur. J. Biochem. 230*, 127–132.

(11) Switala, J., O'Neil, J. O., and Loewen, P. C. (1999) Catalase HPII from *Escherichia coli* exhibit enhanced resistance to denaturation. *Biochemistry 38*, 3895–3901.

(12) Chelikani, P., Donald, L. J., Duckworth, H. W., and Loewen, P. C. (2003) Hydroperoxidase II of *Escherichia coli* exhibits enhanced resistance to proteolytic cleavage compared to other catalases. *Biochemistry 42*, 5729–5735.

(13) Olson, L. P., and Bruice, T. C. (1995) Electron tunneling and *ab initio* calculations related to the one-electron oxidation of NAD(P)H bound to catalase. *Biochemistry 34*, 7335–7347.

(14) Sicking, W., Korth, H.-G., de Groot, H., and Sustmann, R. (2008) On the functional role of a water molecule in clade 3 catalases: A proposal for the mechanism by which NADPH prevents the formation of Compound II. *J. Am. Chem. Soc. 130*, 7345–7356.

(15) Switala, J., and Loewen, P. C. (2002) Diversity of properties among catalases. *Arch. Biochem. Biophys. 401*, 145–154.

(16) von Ossowski, I., Mulvey, M. R., Leco, P. A., Borys, A., and Loewen, P. C. (1991) Nucleotide sequence of *Eschericia coli katE*, which encodes catalase HPII. *J. Bacteriol. 173*, 514–520.

(17) Kunkel, T. A., Roberts, J. D., and Zakour, R. A. (1987) Rapid and efficient site-specific mutagenesis without phenotypic selection. *Methods Enzymol. 154*, 367–382.

(18) Sanger, F. S., Nicklen, S., and Coulson, A. R. (1977) DNA sequencing with chain-terminating inhibitors. *Proc. Natl. Acad. Sci. U.S.A. 74*, 5463–5467.

(19) Rørth, H. M., and Jensen, P. K. (1967) Determination of catalase activity by means of the Clark oxygen electrode. *Biochim. Biophys. Acta 139*, 171–173.

(20) Layne, E. (1957) Spectrophotometric and turbidimetric methods for measuring proteins. *Methods Enzymol. 3*, 447–454.

(21) Bravo, J., Verdaguer, N., Tormo, J., Betzel, C., Switala, J., Loewen, P. C., and Fita, I. (1995) Crystal structure of catalase HPII from *Escherichia coli*. *Structure 3*, 491–502.

(22) Bravo, J., Maté, M. J., Schneider, T., Switala, J., Wilson, K., Loewen, P. C., and Fita, I. (1999) Structure of catalase HPII from *Escherichia coli* at 1.9 Å resolution. *Proteins 34*, 155–166.

(23) Collaborative Computational Project, Number 4. (1994) The CCP4 Suite: Programs for protein crystallography. *Acta Crystallogr. D50*, 760–763.

(24) Murshudov, G. N., Vagin, A. A., and Dodson, E. J. (1997) Refinement of macromolecular structures by the maximum-likelihood method. *Acta Crystallogr. D53*, 240–255.

(25) Emsley, P., and Cowtan, K. (2004) Coot: Model-building tools for molecular graphics. *Acta Crystallogr. D60*, 2126–2132.

(26) Sevinc, M. S., Switala, J., Bravo, J., Fita, I., and Loewen, P. C. (1998) Truncation and heme pocket mutations reduce production of functional catalase HPII in *Escherichia coli*. *Protein Eng. 11*, 549–555.

(27) Chelikani, P., Carpena, X., Perez-Luque, R., Donald, L. J., Duckworth, H. W., Switala, J., Fita, I., and Loewen, P. C. (2005) Characterization of a large subunit catalase truncated by proteolytic cleavage. *Biochemistry 44*, 5597–5605.

(28) Maté, M. J., Sevinc, M. S., Hu, B., Bujons, J., Bravo, J., Switala, J., Ens, W., Loewen, P. C., and Fita, I. (1999) Mutants that alter the covalent structure of catalase hydroperoxidase II from *Escherichia coli*. *J. Biol. Chem. 274*, 27717–27725.

(29) Carpena, X., Soriano, M., Klotz, M., Duckworth, H. W., Donald, L. J., Melik-Adamyan, W., Fita, I., and Loewen, P. C. (2003) Structure of the clade 1 catalase, CatF of *Pseudomonas syringae*, at 1.8 Å resolution. *Proteins 50*, 423–426.

(30) Mate, M. J., Zamocky, M., Nykyri, L. M., Herzog, C., Alzari, P. M., Betzel, C., Koller, F., and Fita, I. (1999) Structure of catalase-A from *Saccharomyces cerevisiae*. *J. Mol. Biol. 268*, 135–149.

(31) Loewen, P. C., Carpena, X., Rovira, C., Ivancich, A., Perez-Luque, R., Haas, R., Odenbreit, S., Nicholls, P., and Fita, I. (2004) Structure of *Helicobacter pylori* catalase, with and without formic acid bound, at 1.6 Å resolution. *Biochemistry 43*, 3089–3103.

(32) Chiu, J. T., Loewen, P. C., Switala, J., Gennis, R. B., and Timkovich, R. (1989) Proposed structure for the prosthetic group of the catalase HPII from *Escherichia coli*. *J. Am. Chem. Soc. 111*, 7046–7050.

(33) Domínguez, L., Sosa-Peinado, A., and Hansberg, W. (2010) Catalase evolved to concentrate H_2O_2 at its active site. *Arch. Biochem. Biophys. 500*, 82–91.

(34) Kooter, I. M., Pierik, A. J., Merkx, M., Averill, B. A., Moguilevsky, N., Bollen, A., and Wever, R. (1997) Difference Fourier transform infrared evidence for ester bonds linking the heme group in myeloperoxidase, lactoperoxidase, and eosinophil peroxidase. *J. Am. Chem. Soc. 119*, 11542–11543.

(35) Blair-Johnson, M., Fiedler, T., and Fenna, R. (2001) Human myeloperoxidase: Structure of a cyanide complex and its interaction with bromide and thiocyanate substrates at 1.9 Å resolution. *Biochemistry 40*, 13990–13997.

(36) Ochi, H., Hata, Y., Tanaka, N., Kakudo, M., Sakurai, T., Aihara, S., and Morita, Y. (1983) Structure of rice ferricytochrome c at 2.0 Å resolution. *J. Mol. Biol. 166*, 407–418.

(37) Pearson, A. R., Elmore, B. O., Yang, C., Ferrara, J. D., Hooper, A. B., and Wilmot, C. M. (2007) The crystal structure of cytochrome P460 of *Nitrosomonas europaea* reveals a novel cytochrome fold an heme-protein cross-link. *Biochemistry 46*, 8340–8349.